

# A Novel Solid-State Oxygen Sensor

*Arthur E. Colvin, Jr., Terry E. Phillips, Joseph A. Miragliotta, R. Ben Givens,  
and C. Brent Barger*

**A** unique solid-state optical sensor configuration has been developed that can serve as a development platform for a host of chemical and biochemical sensors in either gaseous or liquid environments. We describe the first adaptation of the device to oxygen sensing via fluorescence quenching and note the clear and distinct advantages over existing electrochemical and more recent fiber-optic methods. This platform technology features greatly enhanced energy efficiency, high sensitivity, low power consumption, ease of miniaturization, low cost, high-volume manufacturability using standard methods, very fast response/recovery profiles, and high reliability.

## INTRODUCTION

Oxygen is a critical component in many areas such as the environment, industry, respiration, aerobic metabolism, energy, medicine, and agriculture. Although the environmental supply of O<sub>2</sub> is plentiful, the cost of preparing, processing, packaging, and using O<sub>2</sub> is considerable. With the use of inexpensive, high-performance O<sub>2</sub> sensors, the O<sub>2</sub> losses that accompany many applications can be reduced through tighter feedback control, thereby lowering costs. For example, a significant fraction of the annual operating budget of U.S. hospitals is consumed by O<sub>2</sub> supply, handling, and delivery. Effective sensor strategies and control have the potential of reducing this expense. In addition to being able to determine gaseous concentrations, it is often important to measure the amount of O<sub>2</sub> dissolved in water. One of our main interests is the concentration of dissolved O<sub>2</sub> in the oceans and other bodies of water.

Historically, techniques for measuring O<sub>2</sub> have included gas chromatography, mass spectrometry, paramagnetic resonance, and electrochemical techniques.

Of these, only the electrochemical technique, as embodied in the Clark electrode (developed in the 1940s), is currently used for aqueous applications. It is also used in gaseous-state O<sub>2</sub> measurements. However, since O<sub>2</sub> must diffuse through a membrane and a liquid electrolyte in order to be measured, the response time of this type of sensor is quite slow—on the order of a minute. In addition, because the electrolyte is consumed during the measurement process, it must be periodically replaced. Other disadvantages include the electrode's tendency to drift, its inability to tolerate large pressure differentials, and its consumption of O<sub>2</sub> in the measurement process, making low-volume and low-concentration measurements impractical.

Within the past decade, the use of solid-state, fluorescence-based sensors for O<sub>2</sub> determinations has received considerable attention because of the high sensitivity, selectivity, and affordability provided by many indicator molecule/polymer matrix systems.<sup>1</sup> In these sensors, modifications to the intensity and

lifetime (i.e., quenching) of a fluorescent species occur after direct (or indirect) interaction with an analyte gas species. In recent years, metal complexes containing transition metals such as Ru and Os have become an important class of sensor materials for gaseous O<sub>2</sub>.<sup>2</sup> In part, the potential afforded by these materials in optically based sensors stems from their long fluorescent lifetimes (10<sup>-7</sup> to 10<sup>-5</sup> s), large fluorescent quantum yields (0.1 to 0.5), and intense absorption in the visible and near-IR range of the spectrum. More importantly, molecular tailoring provides an ability to design metal complex systems that are sensitive to environmental agents such as O<sub>2</sub> and can be incorporated into a molecularly selective polymer matrix such as silicone.<sup>3</sup>

## SENSING TECHNIQUE

A number of optical procedures can be used to detect either the intensity or temporal characteristics of the resulting fluorescence. In the case of the Ru- and Os-based O<sub>2</sub> sensing dye complexes, the microsecond-scale lifetimes associated with the emission process allow time-resolved measurements of the dye's fluorescence to be made conveniently. To date, Ru(II) complexes have been shown to possess some of the longest lifetimes and largest quantum yields, as well as the chemical stability necessary for O<sub>2</sub> sensing applications based on fluorescence quenching. The complex used in these studies is ruthenium(II)tris((4,7-diphenyl)-1,10-phenanthroline) perchlorate. Upon exposure of the metal complex to gaseous O<sub>2</sub>, the dipolar interaction between the two species perturbs (quenches) the indicator molecule's optically pumped excited state,<sup>2</sup> thus enhancing the pathway for the nonradiative relaxation mechanism and reducing the optical emission intensity. In homogeneous media, the variation with O<sub>2</sub> concentration of both the lifetime  $\tau$  and intensity  $I$  of the luminescence is described by the Stern-Volmer equation<sup>4</sup>

$$\frac{I_0}{I} = \frac{\tau_0}{\tau} = 1 + k_{sv} p_{O_2}, \quad (1)$$

where  $p_{O_2}$  is the O<sub>2</sub> partial pressure,  $k_{sv}$  is the Stern-Volmer quenching constant, and  $I_0$  and  $\tau_0$  are the intensity and lifetime of the luminescence in the absence of O<sub>2</sub>, respectively.

An approach that has proved useful in monitoring the variation in lifetime with gas exposure is a frequency modulation technique that relies on measuring the phase shift of the fluorescence emission relative to the excitation light source.<sup>5</sup> In this approach, the excitation light source is modulated at a fixed frequency whose period is comparable to the lifetime of the emission. The modulated emission is detected with a

conventional detector (photodiode or photomultiplier) and analyzed with a phase-sensitive detector, for example, a lock-in amplifier. The phase angle  $\theta$  is related to the lifetime through the following expression:

$$\tan \theta = 2\pi f\tau, \quad (2)$$

where  $\tau$  is the lifetime of the emission and  $f$  is the frequency of the modulation. In the case where  $\tau_1$  and  $\tau_2$  are the lifetimes of the quenched and unquenched species respectively, the frequency where the maximum phase difference occurs is  $f = (1/2\pi)(\tau_1\tau_2)^{-1/2}$ . For most metal complexes used to date, lifetimes are on the order of a few microseconds, and typical modulation frequencies are in the 10<sup>4</sup> to 10<sup>5</sup> Hz range. These frequencies are easily achieved with solid-state light-emitting diodes (LEDs).

As shown in Eq. 1, the increase in analyte pressure quenches the given ratio of intensities and lifetimes in a linear manner, provided the interactions between the metal complex and surrounding polymer matrix are sufficiently uniform. Practically, however, the immobilization of the indicator molecule in a supporting matrix typically creates a heterogeneous environment that results in deviations from the linear behavior expressed in Eq. 1. In these polymer systems, the intensity variations display a markedly nonlinear response over the range of O<sub>2</sub> pressures used. However, appropriate modeling of the distribution of dipolar interactions in the heterogeneous matrix environment has been shown to fit accurately to experimental results.<sup>6,7</sup>

## A UNIQUE AND ENABLING SENSOR CONFIGURATION

Fluorescence-based optical sensors can be configured in a variety of ways depending on the intended application. A popular configuration is to coat the end of an optical fiber with a film of polymer containing an immobilized fluorescent indicator, as depicted in Fig. 1. In this embodiment, the fiber is bifurcated; the excitation light is directed into the sensing film through one branch of the fiber, and the fluorescent signal is directed back to a detection system through the other branch. This type of sensor is easily inserted into a catheter to make measurements in the body or other difficult-to-reach places. A disadvantage of this configuration arises when a fast response is required and the sensing film is made thin to achieve this goal; the overall optical throughput drops significantly. To compensate for this decreased efficiency, higher-energy (more expensive) sources and more sensitive optical detectors are required. Higher-energy sources often result in accelerated photobleaching of the indicator molecules. The inefficiency results from the fact that

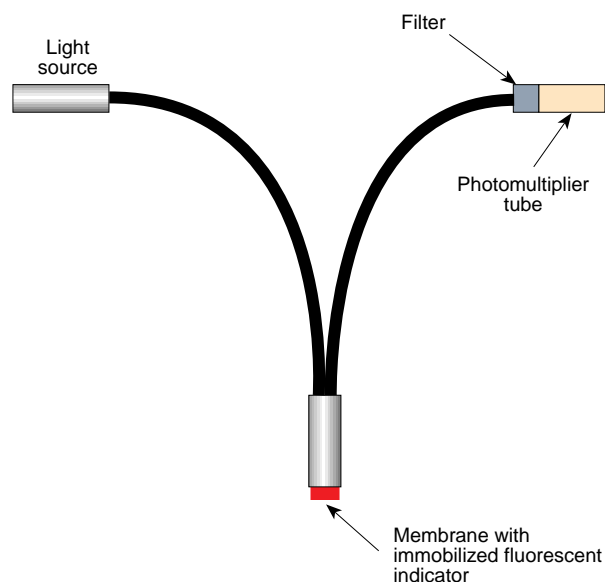


**Figure 1.** Typical configuration of a bifurcated fiber-optic sensor.

the same dimension controlling the sensor response time, namely, the film thickness, also affects the magnitude of the signal available from the fluorescent molecular complex.

A more desirable configuration is one in which the dimension responsible for the optical absorption and the subsequent fluorescence is decoupled from the dimension in which the analyte of interest must diffuse into the sensing element. Light absorption is described by Beer's law, which states that light is absorbed exponentially as a function of distance  $r$  into the medium with an absorption constant  $\lambda$ ; i.e.,  $I = I_0 \exp(-\lambda r)$ . Diffusion is described by Fick's law (see Eq. 3). A design that decouples the Beer's and Fick's law dimensions in a fluorescence sensor is depicted in Fig. 2. A partially assembled sensor is shown in Fig. 3. Here, the excitation light source is a small, inexpensive, edge-emitting LED (200  $\mu\text{m}$  on an edge) positioned in a pocket formed in an optical filter. The polymer, with immobilized fluorescent indicator, is poured around the LED until it is flush with the top of the diode. Light emanates from the LED radially throughout the film (which is viewed edge-on in the horizontal dimension in Fig. 2). The analyte, on the other hand, reaches the indicator complex by diffusion from

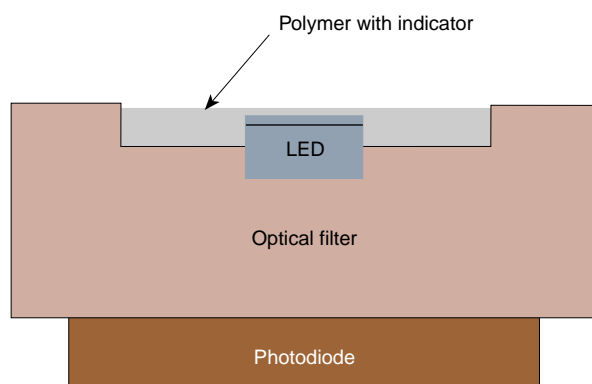


**Figure 2.** Schematic drawing of the newly invented fluorescence sensor that separates the dimension of absorption of excitation light from the dimension that governs response time (diffusion); that is, the platform decouples Beer's law from Fick's law.

above (vertically downward in Fig. 2). Consequently, the polymer thickness can be decreased for faster sensor response without changing the radial dimension, which primarily determines how much light will be absorbed to produce fluorescence. The practical lower limits of this size reduction are set by the dimension of the LED's emitting surface, the LED's emission angle, and scattering effects in the membrane itself.

Both the LED and the polymer film are placed on top of an optical filter. The purpose of this filter is to absorb any scattered excitation light, while allowing the longer-wavelength fluorescent light to pass through to the photodiode detector. As mentioned earlier, either the intensity or the temporal behavior of the fluorescent

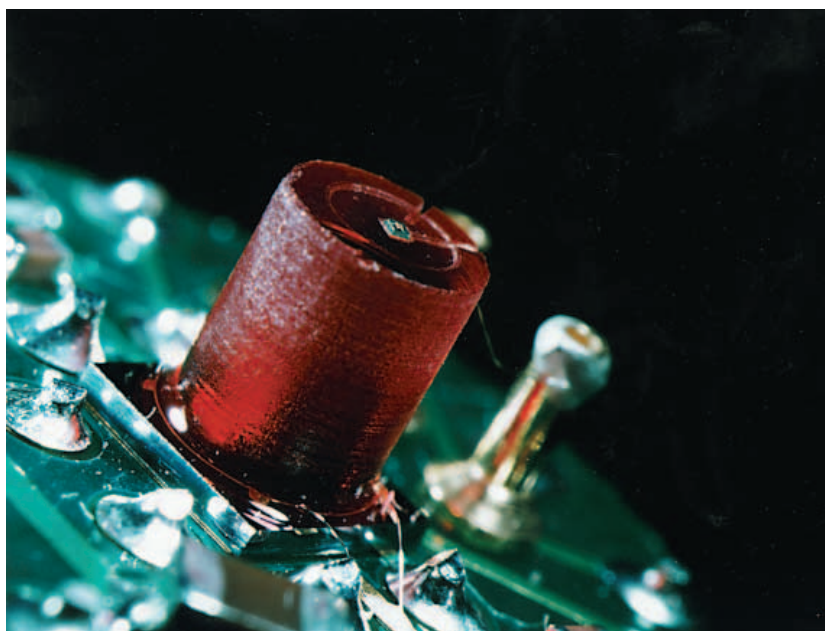


**Figure 3.** Partially assembled sensor showing the LED sitting in a shallow well in an optical filter that will eventually contain the polymer with immobilized indicator complex. For reference, the red filter has a diameter of 0.1 in.

signal can be used to determine the analyte concentration. For some applications, the easily implemented fluorescent intensity measurement is more than adequate. However, in applications where the LED optical output, or the bleaching or leaching of the fluorescent indicator might be an issue, this simple technique is not adequate. Intensity measurements do not distinguish between these types of changes and a change in the analyte concentration. Temporal measurements are accomplished by modulating the supply current to the LED and detecting the phase response of the fluorescent signal with a phase-sensitive lock-in amplifier. This phase measurement mode has the advantage that the result is, within limits, independent of the amplitude of the LED light and is also independent of the amount of indicator in the film. Furthermore, measurements are unaffected by ambient light. Therefore, as the LED ages and its output decreases, or if the indicator is bleached or leached out of the film, the response of the sensor to the analyte does not change and the sensor does not have to be continually recalibrated.

The patent for this platform, which can be exploited for a number of analytes, is owned by Arthur E. Colvin, Jr., and licensed to Process Technologies, Inc. Currently, APL and Process Technologies are developing an O<sub>2</sub> sensor that uses a ruthenium–phenanthroline complex immobilized in a silicone polymer. The optical excitation peak of this complex corresponds well with the blue light obtained from a silicon carbide or gallium nitride LED. The peak fluorescence emission occurs well into the red and is easily separated from the excitation light with a simple glass filter.

## APPLICATIONS

Applications for O<sub>2</sub> sensors are numerous. In the medical field, blood gas sensors are needed for bedside monitors and noninvasive checks elsewhere. Ventilators use sensors to control respiratory cycles. In operating rooms, sensors are used to control the mixing of gases such as O<sub>2</sub> and N<sub>2</sub>. Burn centers use oxygen-control sensors in recovery units. The military needs O<sub>2</sub> sensors to monitor confined spaces on ships, armored personnel vehicles, and cockpits. Oxygen is monitored in reactor cooling water. NASA monitors O<sub>2</sub> and other gases in capsules and other areas in spacecraft. Though not all-inclusive, Table 1 contains many other applications for sensors of this gas. In general, commercial and military applications overlap in many areas, especially in the medical, nuclear, and environmental fields.

At APL, we plan to use this sensor in an aqueous environment. This use presents challenges that have not been encountered previously. In particular, combined pressure and temperature effects on the transduction mechanism, stability, and lifetime of the polymeric membrane and indicator in an aqueous environment, and

simple packaging issues must be addressed for this sensor to be used for the intended environmental applications.

The O<sub>2</sub> sensors discussed in this article were made by Process Technologies, Ijamsville, Maryland. Waterproofed prototypes of the sensors have been produced and are currently being tested. Two applications to measure dissolved O<sub>2</sub> are being pursued. The first is a deep-ocean O<sub>2</sub> sensor. The authors are working with Guy J. Farruggia and John C. Neal of APL's Submarine Technology Department on this project, which is sponsored by the Independent Research and Development (IR&D) Program's Photonics and Electro-Optics Thrust Area under Harry K. Charles, Jr. The second application is to measure dissolved O<sub>2</sub> in the Chesapeake Bay in parallel with marine toxicity measurements being made by Dennis Burton of the University of Maryland Wye Institute. His current instrumentation includes a Clark electrode for O<sub>2</sub> measurements. By using our solid-state device alongside the Clark electrode in Burton's experiments, direct comparisons can be made to validate the utility of the new sensor in a field situation. On the second project, we are working with Daniel G. Ondercin and Charles C. Sarabun, Jr., also of the Submarine Technology Department. This project is sponsored by the IR&D Environmental Thrust Area under Harold I. Heaton.

## SENSOR TESTS IN A GASEOUS ENVIRONMENT

Most of the applications listed in Table 1 require measurements to be made of O<sub>2</sub> concentrations in the 1 to 760 Torr (1 atm) range. Figure 4 shows that the device can cover that full range. As the pressure decreases, the sensitivity of the sensor increases. Below 10 Torr, the intensity response is nearly linear (see inset to Fig. 4). Although linearity is not an essential characteristic of a sensor design, it is often convenient, and

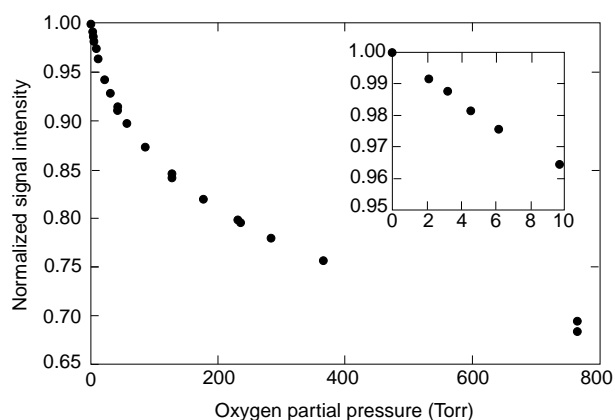


**Figure 4.** Plot showing the signal intensity normalized to the 0% O<sub>2</sub> signal intensity ( $I/I_0$ ) as a function of O<sub>2</sub> pressure from 0 to 760 Torr. The inset presents an enlarged view of the 0 to 10 Torr region, which shows a nearly linear response to O<sub>2</sub> pressure.

**Table 1. Applications for oxygen sensors.**

| Area                 | Application  |
|----------------------|--|
| Military/government  |  |
| Confined space       | Shipboard monitoring, APV, cockpit                   |
| Nuclear power        | Reactor cooling water                                |
| NASA                 | Capsule monitoring                                   |
| Toxic waste          | Field monitors                                       |
| Medical              |  |
| Blood gas            | Bedside monitors, noninvasive checks                 |
| Ventilators          | Control respiration cycle                            |
| Operating rooms      | N <sub>2</sub> -O <sub>2</sub> mixing                |
| Burn units:          | O <sub>2</sub> control recovery units                |
| Environmental        |  |
| Air pollution        | EPA monitoring                                       |
| Ground/surface water | BOD determination, pollution monitoring              |
| Municipal water      | BOD, water quality, waste treatment plants           |
| Industrial processes |  |
| Biological           | Fermentation, synthesis                              |
| Chemical             | Petroleum cracking, catalysis                        |
| Boiler water         | Corrosion control                                    |
| Nuclear plants       | Cooling water monitors                               |
| Food/brewing         | Carbonation, packaging, process control, formulation |
| Semiconductor        | Plating processes                                    |
| Gas suppliers        | O <sub>2</sub> , CO <sub>2</sub> suppliers           |
| Health safety        |  |
| Occupational         | Mines, silos, tunnels, manhole monitors              |
| Building             | HVAC monitors/controls                               |
| Inerting             | Explosion control                                    |
| Transportation       |  |
| Perishables          | Container monitors                                   |
| Law enforcement      | Immigration control                                  |
| Ship safety          | Environmental/explosion control                      |
| Auto emissions       | Exhaust sensors                                      |
| Miscellaneous        |  |
| Scuba diving         | Gas recovery systems                                 |
| Aquariums            | Commercial fish tanks, aquaculture                   |

Note: BOD = biological oxygen demand; APV = armored personnel vehicle.

intensity change over the full pressure range of about 32%. We have since been able to improve this result to about 85% by altering the procedure by which the indicator complex is immobilized in the polymer matrix. We expect further improvement in the future.

Figures 5 and 6 illustrate results obtainable using the intensity and phase methods of O<sub>2</sub> measurement, respectively. The intensity measurements have their greatest sensitivity in the lowest-frequency range, with peak sensitivity occurring at 0 Hz. Figure 5 shows that for this particular device, the intensity was quenched by about 60% when exposed to an atmosphere of O<sub>2</sub> relative to that in an atmosphere of an inert gas; in this case, Ar was used. Identical results were obtained when N<sub>2</sub> was substituted for Ar. The intensity level is, of course, directly proportional to the LED drive current amplitude. Therefore, decreasing the drive current lowers the fluorescence output proportionately. On the other hand, Fig. 6 demonstrates that the phase sensitivity increases with frequency in accordance with Eq. 2. Significantly, changes in the LED intensity have little or no effect on the value of the measured phase as shown in the figure where data for 4-mA drive current is observed to possess virtually the same values as data for 6-mA current. This latter observation has at least one important ramification; that is, as the LED ages and decreases its output for an unaltered current input, the change in phase will still only depend upon the level of O<sub>2</sub> present. This means that using the phase measurements instead of intensity is advantageous because recalibration will not be required over the useful lifetime of the sensor. It should be noted that the results shown in Figs. 5 and 6 were obtained using an externally

mounted LED, instead of the internal LED shown in Figs. 2 and 3. When the internal LED is modulated at high frequencies (>1 kHz), the capacitive coupling of the LED drive voltage to the photodiode output

it is possible that the linearity in this system can be extended to higher-pressure regions by altering the concentration of indicator in the polymer and/or the nature of the immobilizing matrix. Figure 4 also shows an

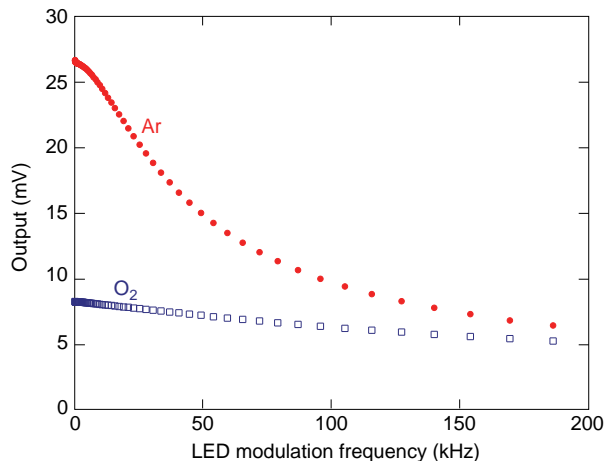


**Figure 5.** Intensity measurements as a function of frequency using a lock-in amplifier demonstrating that the greatest sensitivity in intensity measurements is at 0 Hz.

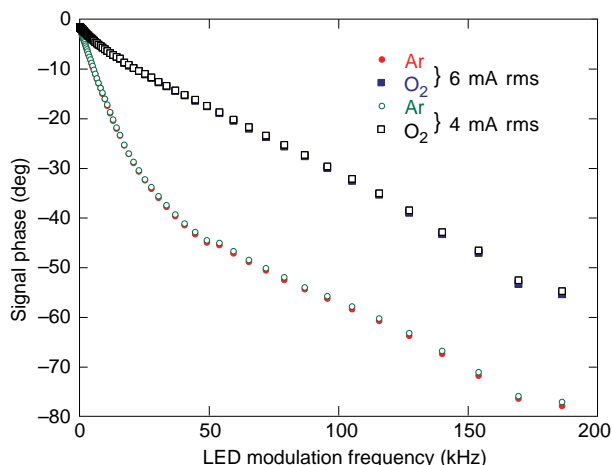


**Figure 6.** Phase measurements as a function of frequency using a lock-in amplifier. Data for both pure oxygen and pure Ar are virtually the same for LED drive currents of 4 and 6 mA. In fact, it is difficult to see that there are really two sets of data for both O<sub>2</sub> and Ar.

complicates the phase determination of the signal. This coupling can be easily compensated at any given frequency. However, for the purpose of showing the intensity and phase over a broad frequency range, it was necessary to use an external LED to eliminate the capacitive coupling completely.

As expected, the fluorescence process is sensitive to temperature changes. Measurements made over a range of temperatures between 23 and 33°C showed a change of  $-0.5\%/^{\circ}\text{C}$  for intensity and  $0.06\%/^{\circ}\text{C}$  for phase measurements. This sensitivity is easily compensated for electronically using an internal thermistor.

New applications of oxygen sensing in health care and elsewhere will be enabled by devices that demonstrate a subsecond response to change in the O<sub>2</sub> concentration. As indicated earlier, faster responses can be achieved for the sensor being discussed here by mak-

ing the polymer membrane thinner. Oxygen sensors currently on the market have response times on the order of tens of seconds. Figure 7 shows the change in response time using intensity data when the atmosphere is changed from Ar to O<sub>2</sub>. (These data are uncompensated for the time it takes to change the atmosphere external to the sensor, which is not instantaneous.) About 0.9 s elapsed from the 90% to 10% sensor response. Another experiment was set up allowing the prediction of response time for various thicknesses of the actual polymer/indicator film formulation. Using an Ar laser for excitation and a thin film of Ru complex immobilized in silicone on a glass slide, we measured response times on the order of 100 ms. These response times will allow one to follow the O<sub>2</sub> level during the inhale/exhale breathing cycle and, thus, be very useful for important medical applications, where analysis of the variations in exhaled gases during a single breathing cycle provides diagnostic information.

The diffusion process, which controls the response time, was modeled using the one-dimensional diffusion equation, also known as Fick's second law:

$$D\partial^2 C(x,t)/\partial x^2 = \partial C(x,t)/\partial t, \quad (3)$$

where  $D$  is the diffusion constant of O<sub>2</sub> in silicone in this case,  $t$  is time, and  $C$  is concentration, which is a function of position  $x$  and time. In solving Eq. 3 for a relevant set of circumstances, the sensor is assumed to be a plane sheet of polymer with immobilized indicator. The sheet is of infinite extent in two dimensions and of thickness  $d$  in the  $x$  dimension. At time  $t = 0$ , the concentration is uniform inside the sheet and possesses a value of  $C_i$ ; outside the sheet, the concentration is also uniform with a value of  $C_0$ . One surface of the sheet is located at  $x = 0$ , and the other is at  $x = d$ . In other words, at  $t = 0$ , for  $0 < x < d$ ,  $C(x,0) = C_i$ , and for

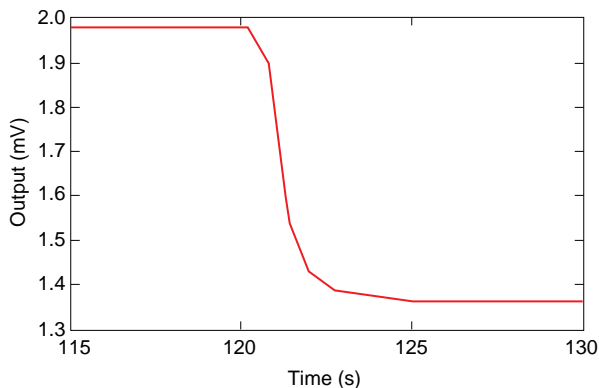


**Figure 7.** Signal measured as a function of time showing the sensor response upon changing the gaseous environment of the sensor from 100% Ar to 100% O<sub>2</sub>.



$x > d$ ,  $C(x,0) = C_0$ . The conditions are such that for  $x > d$ ,  $C(x,t)$  always remains constant at  $C_0$ . At  $x = 0$ , we set  $\partial C/\partial x = 0$  for  $t > 0$ . The condition of setting the partial derivative to zero means physically that no net diffusion of analyte occurs at  $x = 0$ . Diffusion begins at  $t = 0$ . Crank<sup>8</sup> solves precisely this problem, giving both a general solution and one for short times (i.e., when  $Dt/d^2$  is small, which in this case is even as large as 5 or so). The solution for small  $t$  is given in terms of an infinite series as follows:<sup>8</sup>

$$\frac{C - C_1}{C_0 - C_1} = \sum_{n=0}^{\infty} (-1)^n \operatorname{erfc} \frac{(2n+1)d - x}{2\sqrt{Dt}} + \sum_{n=0}^{\infty} (-1)^n \operatorname{erfc} \frac{(2n+1)d + x}{2\sqrt{Dt}}, \quad (4)$$

where  $\operatorname{erfc}(z)$  is the standard complementary error function. Figure 8 presents a series of graphical results at various positions  $x$  for a maximum normalized concentration of 1, a film thickness of  $d = 70 \mu\text{m}$ , and a diffusion constant<sup>9</sup> of  $D = 1.2 \times 10^{-5} \text{ cm}^2/\text{s}$ . This diffusion constant pertains to  $\text{O}_2$  diffusion in vulcanized poly(oxydimethylsilylene), which should be close to the silicone polymer we use to make the  $\text{O}_2$  sensor. We note, however, that mathematically the solutions are quite sensitive to the values of  $D$  and  $d$ . (Even for times as long as 10 s, the summations in Eq. 4 converge easily by the  $n = 4$  term. Our sums were carried out beyond this.) Considering that the data in Fig. 7 represent an experimental situation in which light from all positions in the film is integrated at the photodetector, that the diffusion constant is not known with great certainty, and that the film thickness was not well characterized, the calculations agree quite well with experiment.

## FUTURE PLANS

Our future plans for this unique sensor architecture extend along two paths. Following our evaluation of the device as an  $\text{O}_2$  sensor in both gaseous and liquid environments, we will continue to explore its application to other important analytes. This effort will primarily involve designing indicator/polymer matrix systems for installation onto the engineering platform. Our second effort will be to explore fully the engineering parameters of the existing design for total optimization. This information will help identify the important issues relevant

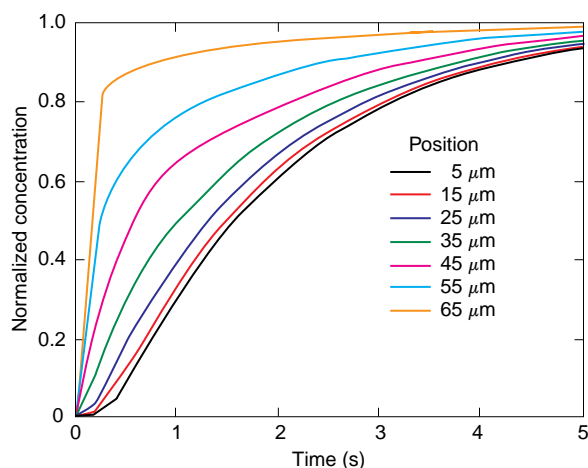


**Figure 8.** Calculated  $\text{O}_2$  concentration as a function of both position in a polymer film and time after the gaseous environment is “switched on” at  $t = 0$ . The film is  $70 \mu\text{m}$  thick with an  $\text{O}_2$  diffusion constant<sup>9</sup> of  $1.2 \times 10^{-5} \text{ cm}^2/\text{s}$ .

to designing a monolithic chip, thereby integrating chemistry, optics, and signal processing to a single silicon embodiment.

## REFERENCES

- Lieberman, R. A., and Wlodarczyk, M. T. (eds.), *Chemical, Biochemical, and Environmental Sensors*, Society for Optical Engineering, Bellingham, WA, p. 1172 (1989).
- Demas, J. N., and DeGraff, B. A., “Design and Applications of Highly Luminescent Transition Metal Complexes,” *Anal. Chem.* **63**, 829A-837A (1991).
- Carraway, E. R., Demas, J. N., deGraff, B. A., and Bacon, J. R., “Photophysics and Photochemistry of Oxygen Sensors Based on Luminescent Transition-Metal Complexes,” *Anal. Chem.* **63**, 337-342 (1991).
- Bacon, J. R., and Demas, J. N., “Determination of Oxygen Concentrations by Luminescence Quenching of a Polymer-Immobilized Transition-Metal Complex,” *Anal. Chem.* **59**, 2780-2785 (1987).
- Bambot, S. B., Holavanahail, R., Lakowicz, H. R., Carter, G. M., and Rao, G., “Phase Fluorometric Sterilizable Optical Oxygen Sensor,” *Biotech. Bioeng.* **43**, 1139-1145 (1994).
- Carraway, E. R., Demas, J. N., and deGraff, B. A., “Luminescence Quenching Mechanism for Microheterogeneous Systems,” *Anal. Chem.* **63**, 332-336 (1991).
- Draxler, S., Lippitsch, M., Klimant, E. I., Kraus, H., and Wolfbeis, O. S., “Effects of Polymer Matrices on the Time-Resolved Luminescence of a Ruthenium Complex Quenched by Oxygen,” *J. Phys. Chem.* **99**, 3162-3167 (1995).
- Crank, J., *The Mathematics of Diffusion*, Cambridge University Press, Cambridge, England, pp. 44-49 (1975).
- Brandrup, J., and Immergut, E. H. (eds.), *Polymer Handbook*, 2d Ed. Wiley-Interscience, New York, p. II-238 (1975).

ACKNOWLEDGEMENT: We wish to acknowledge Dr. John Gerig for his assistance in designing and testing the oxygen sensor’s electronics.

## THE AUTHORS



ARTHUR E. COLVIN, JR., is chief scientist at Process Technologies, Inc., Ijamsville, Maryland. He received a B.S. degree in biochemistry from The Virginia Polytechnic Institute in 1979. He took graduate courses in both mathematics and computer science at APL and in biochemical engineering at the University of Maryland in College Park. Since 1979, as an employee of Life Technologies, Inc., and later at the Cerex Corporation, Mr. Colvin has designed and developed more than 30 commercial products for the biotechnology industry, resulting in 14 U.S. and foreign patents. His research interests include optics-based chemical and biochemical sensors, chemical signal transduction strategies, biocompatible materials, analyte recognition, and microfabrication.



TERRY E. PHILLIPS is a chemist in the Sensor Science Group of the Milton S. Eisenhower Research Center at APL. He received a B.A. from Susquehanna University in 1970 and a Ph.D. in organic chemistry from The Johns Hopkins University in 1976. After completing postgraduate studies at Northwestern University in low-dimensional organic conductors, he joined APL in 1979. He has studied photoelectrochemical energy conversion; inorganic optical and electrical phase transition compounds; high-temperature superconductors; and material characterization with X rays, nuclear magnetic resonance, mass spectroscopy, and optical spectroscopic techniques. His e-mail address is Terry.Phillips@jhuapl.edu.



JOSEPH A. MIRAGLIOTTA, is a physicist and Senior Staff member in the Sensor Science Group of the Milton S. Eisenhower Research Center at APL. He received a B.S. in physics from Manhattan College in New York in 1982 and an M.S. and Ph.D. in physics from Rensselaer Polytechnic Institute in 1985 and 1987, respectively. After joining Exxon Research and Engineering, he worked on the development of a nonlinear optical program from surface studies pertaining to lubrication and corrosion inhibition at liquid/solid interfaces. Since joining the APL Research Center in 1990, he has developed a nonlinear optical program devoted to the spectroscopic analysis of surfaces, compound semiconductors, and thin-film waveguide devices. Dr. Miragliotta has conducted research in surface-enhanced Raman scattering, photoluminescence of semiconductors, and optical scattering in biomedical systems. He is a member of the American Physical Society, the Optical Society of America, the Materials Research Society, the IEEE, and SPIE. His e-mail address is Joseph.Miragliotta@jhuapl.edu.



R. BEN GIVENS is an Associate Staff member in the Sensor Science Group of the M. S. Eisenhower Research Center at APL. He studied electronics while in the U.S. Army and later obtained an Associate's degree in electronics from the Capitol Radio Engineering Institute. He joined APL in 1965 after working for the Maryland Electronic Manufacturing Company, where he focused primarily on evaluating instrument landing systems. Mr. Givens is the inventor of a Lorentz Force Magnetometer, which is now being developed in the Research Center. His e-mail address is Robert.Givens@jhuapl.edu.





C. BRENT BARGERON earned a Ph.D. degree in physics at the University of Illinois in 1971 and joined APL that year as a member of the Milton S. Eisenhower Research Center. He is currently a member of the Sensor Science Group. Since joining APL, Dr. Barger has focused on solid state physics, light scattering, chemical lasers, arterial geometry, corneal damage from infrared radiation, mineral deposits in pathological tissues, quality control and failure analysis of microelectronic components, electron physics, surface science, and sensor science. His e-mail address is Brent.Bargeron@jhuapl.edu.